Earthquakes and Structures, *Vol. 17, No. 5 (2019) 501-510*
DOI: https://doi.org/10.12989/eas.2019.17.5.501

Effectiveness of diagonal shear reinforcement on reinforced concrete short beams

Hakan Ozturk*, Naci Caglar and Aydin Demir

Department of Civil Engineering, Engineering Faculty, Sakarya University, Sakarya, Turkey

(*Received August 8, 2019, Revised October 4, 2019, Accepted October 10, 2019*)

Abstract. In the study, an experimental and numerical study is performed to investigate the efficiency of diagonal shear reinforcement (DSR) on reinforced concrete (RC) short beams. For this purpose, 7 RC short beam specimens were tested under a 4-point loading, and a numerical study is conducted by using finite element method. Additionally, the efficiency of addition of DSR to specimens is observed in the experimental study together with the increase in stirrup spacing. Analysis results are compared in terms of load-displacement behavior and failure modes. As a result of the study, a significant improvement both in shear and displacement capacities of the RC short beams are achieved along with addition of DSR in short beams. Moreover, it is deduced from the numerical results that increasing both the diameter and yield strength of DSR makes a significant contribution to the shear capacity and ductility of shear critical RC members.

Keywords: reinforced concrete; shear; beams; finite element method; numerical simulation

1. Introduction

Reinforced concrete (RC) beams having the ratio of length of shear zone to effective depth (*a/d*) as in between 1.3 and 2.5 are admitted as short beams. The short beams and columns are generally constructed due to architectural and structural compelling reasons and they might be exposed to large cyclic reversals of shear deformations under earthquake loads (Wang *et al*. 2015). Therefore they may experience a quick deterioration of shear strength and stiffness. Stirrup densification proposed widely by many design codes may not be a sufficient solution to resist that shear stresses (Moretti *et al*. 2013, Chang *et al*. 2014). In this cases, these members may perform unexpected brittle shear behavior. Moreover, the bonding between concrete and reinforcement may decrease in densely planted RC members due to difficulties during concrete casting (Wight *et al*. 2012, Demir *et al*. 2016).

In the literature, several alternative techniques have been proposed to improve shear capacity of RC beams. First of all, Corte and Boel (2013), Karayannis and Chalioris (2013), proposed a rectangular spiral reinforcement (RSR) similar to application of spiral transverse reinforcement on RC columns (Fig. 1(a)). In these studies, RC beam specimens were tested under a monotonic four-point loading. Test results deduced that a significant improvement in shear performance of RC beams was observed with the use of RSR. Moreover, Yang *et al*. (2011), conducted an experimental study to investigate effectiveness of spiral-type wire ropes as shear reinforcement (Fig. 1(b)). For that aim, 3 two-span RC T-beams were tested under a four-point

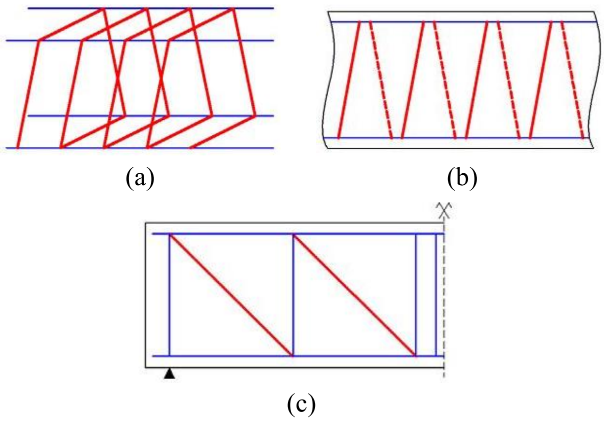

Fig. 1 Alternative shear reinforcement configurations

static loading. According to the test results, the use of wire rope is a convenient technique to enhance ductility of RC beams and it contributes to limit shear crack widths as well. Additionally, in the study of Al-Nasra and Asha (2013), the behavior of swimmer bars as a new type of transverse reinforcement (Fig. 1c) with three types of connection (weld, bolt and u-link bolt) were observed experimentally. Similarly, it is reported in the study that a significant improvement in shear strength of RC beams was experienced.

There are also some different studies in the literature investigating specifically the cyclic performance of diagonal shear reinforcement on different RC members. Firstly, Chalioris *et al*. (2008), conducted an experimental study to observe the effectiveness of crossed inclined bars (*X*-bars) as joint shear reinforcement in exterior RC beam-column joints. Specimens were tested under a cyclic loading. Moreover, in the experimental study of Dirikgil (2014), Dirikgil and Altun (2015), the cyclic performance of

*Corresponding author, Ph.D.
E-mail: hakanozturk@sakarya.edu.tr

ISSN: 2092-7614 (Print), 2092-7622 (Online)

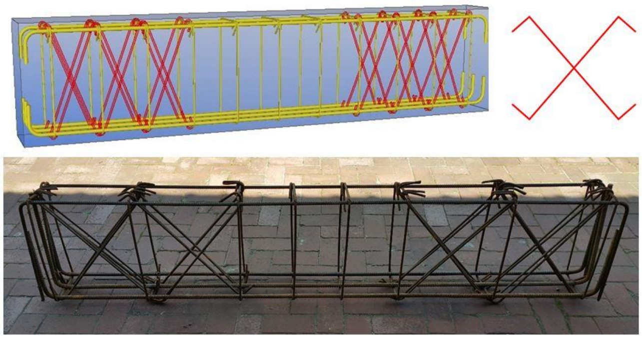

Fig. 2 Application of diagonal shear reinforcement (DSR)

the DSR on RC short columns were investigated. According to the results of both studies, diagonal shear reinforcement exhibited a very improved cyclic performance and enhanced mode of damage.

Additionally, in an existing numerical research of the authors of this study (Demir *et al*. 2016), a new alternative shear reinforcement configuration named as diagonal shear reinforcement (DSR) (Fig. 2) was also proposed to increase shear capacity and ductility of shear critical RC normal beams (*a/d*>2.5). DSR was applied to shear zones between stirrups by adding new diagonal reinforcing bars in the form of steel ties almost perpendicular to shear cracks. It was stated in the study that DSR is an easily applicable, economical and alternative shear reinforcement making a very significant contribution to the bond between concrete and steel reinforcement by reducing density of reinforcement. Moreover, it exhibits very improved performance under a monotonic loading. As a result of the study, it was concluded that DSR provides very significant improvement in both shear and ductility capacity and more ductile behavior is achieved for RC normal beams having insufficient shear reinforcement (Demir *et al*. 2016). However, in the existing study (Demir *et al*. 2016), the performance of proposed DSR shear reinforcement observed only numerically without performing an experimental study. Moreover, the scope of that study was only limited for RC normal beams. Therefore, it is apparent that a new experimental study is needed in order to determine the behavior and efficiency of DSR on RC beams more accurately. Secondly, because DSR is proposed as an alternative shear reinforcement and its cyclic efficiency has been demonstrated on RC columns, the use of DSR on shear critical RC short beams seems obviously much reliable. Because of that reasons in this study, an experimental and numerical study is performed in order to investigate efficiency of DSR reinforcement on RC short beams. For this purpose, 7 RC short beams are tested under a 4 point-loading test setup and a numerical FE study is conducted by using a FE-code ABAQUS (ABAQUS 2018). In the experimental study, efficiency of the existence of DSR on RC short beams is observed. Moreover, effect of yield strength and diameter of DSR is investigated in the numerical study.

2. Experimental study

Table 1 The ratio of tension, compression, stirrup and diagonal shear reinforcement, and angle of DSR.

Specimen	Angle of DSR	Tension Reinforcement	Compression Reinforcement	Stirrup	DSR Horizontal	DSR Vertical
R100	-	0.0053	0.0020	0.0040	-	-
S200	-			0.0020	-	-
SX200	65.30°				0.0008	0.0018
S400	-			0.0010	-	-
SX400	47.30°				0.0013	0.0007
S800	-			0.0005	-	-
SX800	28.50°				0.0016	0.0002

Table 2 Yield and ultimate strengths of reinforcement

Reinforcement	Yield Strength (MPa)	Ultimate Strength (MPa)
Ø8	420	552
Ø12	435	568
Ø16	485	592

In the study, an experimental study is conducted to investigate efficiency of the existing DSR application. For this aim, stirrup spacing and existence of DSR are selected as variable key parameters. However, properties of both compression and tension longitudinal reinforcement and diameter of stirrups are kept constant. DSR is applied to only shear zones of the specimens. The experimental study consists of totally 7 RC short beam specimens, including a reference specimen. They have a different shear reinforcing configuration with same dimensions of 250×500×2250 mm. The ratio of *a/d* is selected as 1.5 for all specimens. The diameter of bottom and top longitudinal bars are 3Ø16 and 2Ø12 respectively. Moreover diameters of both stirrups and DSR are selected as 8 mm with 25 mm concrete cover thickness. The ratios of tension, compression, stirrup and diagonal shear reinforcement, and angle of DSR are given in Table 1.

The similar properties of the specimens such as; dimensions, loading and support locations, and details of longitudinal reinforcement are demonstrated in Fig. 3. All specimens are produced at the same time and tested after 28 days to achieve necessary strength. The 28-day compressive strength of the concrete is obtained from standard tests of cubes and average is determined as 30.3 MPa. Moreover the bottom, top and shear reinforcement diameters are selected as Ø16, Ø12, Ø8 respectively and their yield strengths are reported in Table 2.

The reference specimen is designed with 100 mm stirrup spacing (Fig. 3) according to the requirements given in Turkish Seismic Code 2007 (TSC 2007) and Requirements for Design and Construction of Reinforced Concrete Structures (TS500 2000) to be able to make a comparison with other shear critical members to observe the contribution of DRS on the shear capacity of RC short beams. The remaining 6 specimens are designed as shear critical members with 200, 400 and 800 mm stirrup spacing (s). The detailed drawings of specimen matrix are given in Table 3. The specimens are named in a way that initial letters *R* and *S* are abbreviations of words of “reference” and “specimen” respectively. The numbers given after

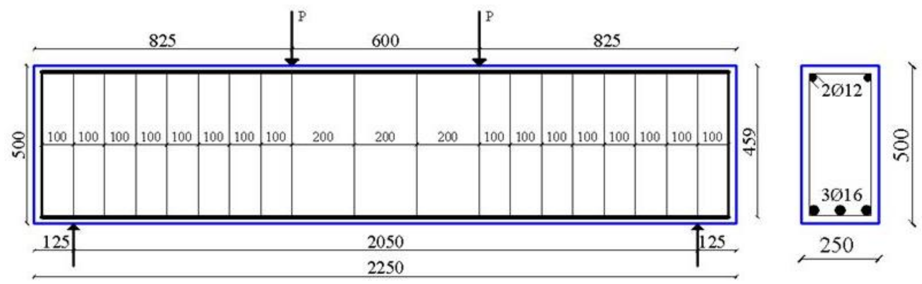

Fig. 3 Details of reference specimen (in mm)

Table 3 Details of the specimen matrix

Specimen ID	Detail of Specimen	Specimen ID	Detail of Specimen
R100 (Reference) (*s*=100 mm)	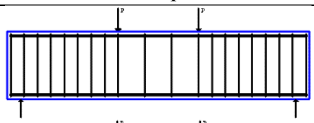	-	-
S800 (*s*=800 mm)	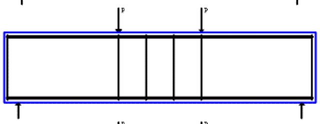	SX800 (*s*=800 mm)	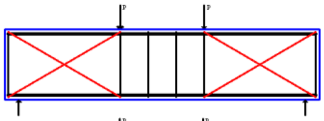
S400 (*s*=100 mm)	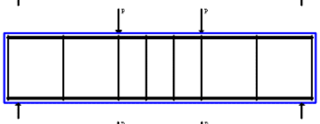	SX400 (*s*=400 mm)	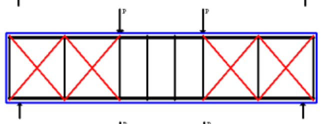
S200 (*s*=200 mm)	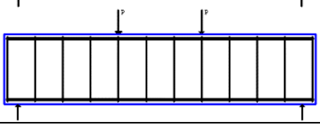	SX200 (*s*=200 mm)	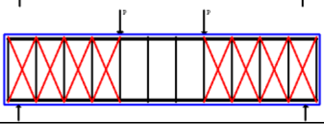

initial letters represent the space of stirrups in millimeter within shear zones. Moreover, "*X*" demonstrates existence of DSR on a relevant specimen.

The dimensional and material properties of S and SX specimens are same with the reference specimen except stirrups spacing and existence of DSR in their shear spans. S800, S400 and S200 are of specimens with 800, 400 and 200 mm stirrup spacing respectively. Moreover, SX800, SX400 and SX200 are specimens with in respective of 800, 400 and 200 mm stirrup spacing. They also contain additional shear reinforcement of DRS in their shear zones (Table 3).

In the literature, RC beams are generally tested under a pin and roller restrained test setups. However, if both supports are designed as pins allowing only rotation, additional tensile stresses cause axial reactions at the supports. Thus, the shear capacity of the member decreases significantly and more brittle shear failure is experienced (Ersoy and Ozcebe 2004). Because of that reasons, both supports are selected as pin restraints in the present study to observe explicitly the contribution of DSR to shear behavior of RC short beams.

The test specimens are subjected to a four-point bending test (Fig. 4). They have a clear span of 2050 mm with 600 mm spacing between the two loading points and a shear span of 700 mm (*a*/*d*=1.5). The specimens are fastened by steel rods and plates from both ends in order to ensure a pinned support condition. A steel spreader beam is placed on the specimens to distribute the applied load equally. The applied load is measured via a load cell and the vertical displacement at the midpoint of the beam is measured by using a linear potentiometer. Moreover, a steel hinge is put between the hydraulic piston and load cell. The load is applied monotonically until the failure of the specimens.

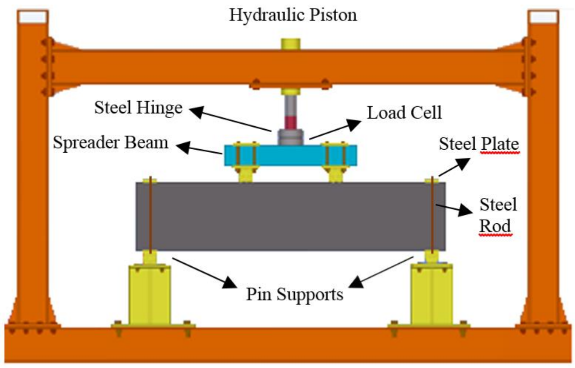

Fig. 4 Test setup

3. Numerical study

It has been proven in the literature that there are several finite element codes are widely used in civil engineering applications and can give very accurate results to model nonlinear behavior of reinforced concrete, composite and masonry structures (Tubaldi *et al*. 2010, Nguyen *et al*. 2016, Hu *et al*. 2017, Panto *et al*. 2017, Luo *et al*. 2019). In the study, numerical simulations are conducted by using ABAQUS (ABAQUS 2018). Which is a general- purpose

Table 4 CDP parameters for ABAQUS material definition of concrete (Demir *et al*. 2016)

Parameter	Taken Value	Description (Lublinear *et al*. 1989)
ψ	56	Dilation angle
ϵ	0,1	Eccentricity
F_{b0}/f_{c0}	1,16	The ratio of initial equibiaxial compressive yield stress to initial uniaxialcompressive yield stress
K_c	0,6667	The ratio of the second stress invariant on the tensile meridian
μ	0,0001	Viscosity parameter

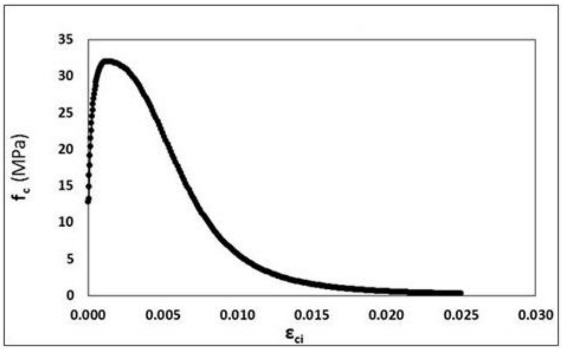

(a) Compressive

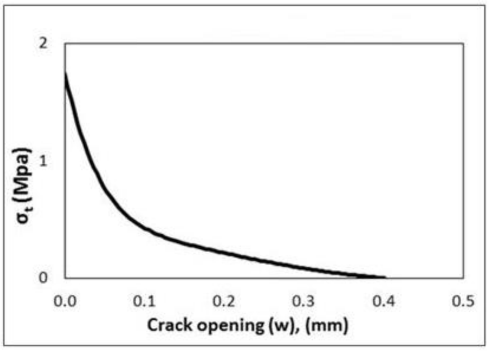

(b) Tensile

Fig. 5 Uniaxial inelastic behavior of concrete

finite element (FE) analysis software that can solve a wide range of linear and nonlinear problems. Concrete damaged plasticity (CDP) model is used to model inelastic material behavior of concrete. CDP provides a general capability for modeling concrete and other quasi-brittle materials in all type of structures (Hibbitt *et al*. 2011). Some basic parameters and their descriptions needed to define CDP model in ABAQUS are depicted in Table 4.

It is required to model the uniaxial compressive and tensile material behaviors of concrete in the CDP model. The numerical compressive and tensile behaviors of concrete are shown in Figs. 5(a) and 5(b) respectively. Reinforcement are modeled by considering elastic and inelastic stress-strain relationships of reinforcing steel. Finite element (FE) type of concrete and reinforcement are selected as an 8-node linear brick (C3D8R) and a 2-node linear 3-D truss (T3D2) respectively. The reinforcement is assumed fully embedded into concrete to simulate interaction between concrete and reinforcing steel. Because of the fact that similar numerical modelling technique is

(a) Reinforcement model

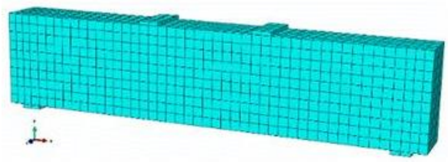

(b) Concrete model

Fig. 6 Meshed numerical FE model

Table 5 Numerically studied parameters of DSR

Parameter	Diameter (mm)		Yield Strength (MPa)	
	Experimental	Numerical	Experimental	Numerical
Diagonal Shear Reinforcement	Ø8	Ø10 Ø12	420	420 / 500

employed in this study, more detailed information can be found in the previous study of the authors (Demir *et al*. 2016) regarding creation of numerical FE model of the tested specimens.

The optimum FE mesh size is found as 50 mm with an aspect ratio of 1 by making a parametric study. One of the meshed numerical FE model is depicted in Fig. 6 for reinforcement and concrete.

After completion of the FE modeling process, numerical verification of the experimentally tested beams are performed. A successful representation of the specimens is achieved on the FE model with a sufficient accuracy in terms of a load-displacement behavior. Subsequently, a numerical parametric study is conducted to investigate effect of the change in diameter and yield strength of DSR on shear performance of RC short beams. Seventeen different FE models are created in total. The investigated parameters are also tabulated in Table 5. The models are named in a way that, for instance A_SX200 DØ10_420; A and S are abbreviation of ABAQUS and Specimen respectively, *X* demonstrates existence of DSR in the model, the integer of 200 represents the space of stirrups (s) in millimeter, DØ10 is stand for the diameter of DSR in millimeter and finally 420 refers to the yield strength of DSR.

On the other hand, the total strain values of concrete and reinforcement are measured determine termination point of the analysis. The limits for crushing strain of the concrete and rupture strain of reinforcing bars are taken into account as 0.018 and 0.06 according to TSC-2007 (TSC 2007) respectively. Once one of those limits are reached, the analyses are terminated (Demir *et al*. 2016).

4. Results and discussions

4.1 Experimental results

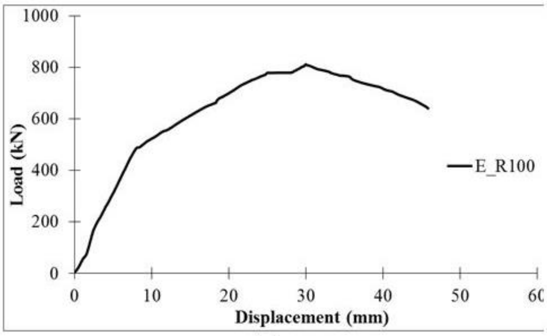

(a)

(b)

Fig. 7 Test results of R100 reference specimen

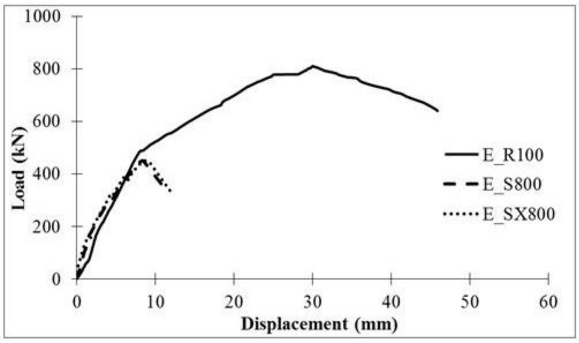

Fig. 8 Load-displacement curves of S800, SX800 and R100

(a) S800

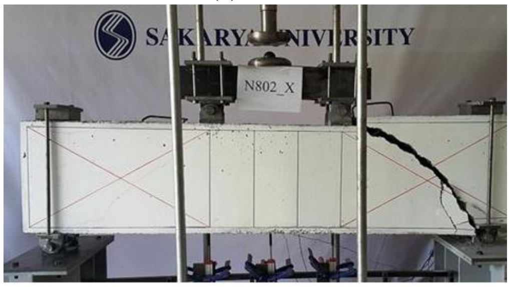

(b) SX800

Fig. 9 Test results of S800 and SX800

All experimental results are demonstrated in terms of load-displacement graphs and crack patterns (Figs. 7-14). Results of the specimens containing only stirrup and DRS reinforcement together with stirrup are compared with the results of the reference specimen. On legend of the graphs; the letters of *E*, *R*, *S* and *X* in the titles of specimens refer to the words of experimental, reference, specimen and existence of DSR reinforcement in the specimen, respectively. Additionally, the integers of 100/200/400/800 represent the space of stirrups in millimeter.

In the test of the reference beam (R100), flexural cracks (at 158 kN) are observed initially at the flexural zone between the loading points. While the number and width of flexural cracks increase, the tension reinforcement started to yield at a point when the applied load reached to 487 kN with 8.6 mm mid-point displacement. The maximum applied load value of 810 kN with 30 mm mid-point displacement was achieved due to strain hardening of the tension bars with contribution of the stirrups to shear capacity of the member. At this point shear cracks were seen at the shear zones. Beyond the maximum applied load value, shear has started to dominate the behavior and the applied load has begun to drop. Since shear capacity of the specimen was exceeded, a sudden brittle shear failure was experienced at the point when applied load reached to 646 kN with 45.6 mm mid-point displacement (Fig. 7).

Additionally, since R100 specimen was designed according to the requirements given in TSC-2007 and TS500 code, it was supposed to perform more ductile failure behavior than experienced in the test. Nevertheless, although the specimen initially performed some ductile behavior with the initiation of flexural crack, shear dominated the behavior and a sudden brittle shear failure was experienced beyond maximum load. It is thought that this behavior stems from the pin restrains preventing the horizontal displacement of the supports. Therefore it can be inferred from the test results that RC shorts beams are shear critical members and designing those members according to criteria enforced in design codes may not be adequate solution to provide a ductile behavior. It can be concluded that a new alternative shear reinforcement is required to be able to make more ductile design of RC short beams.

Secondly, load-displacement graphs of S800, SX800 and R100 specimens are given in Fig. 8. While both S800 and SX800 specimens do not contain any stirrup at their shear zones, DSR nevertheless is included to SX800 specimen (Fig. 9(b)). Because of the fact that due to insufficient shear reinforcement in shear zones, only shear cracks (at 102 kN) occurred on the specimens, and a sudden shear failure is experienced when the applied load is reached to the value of 448 kN with 8.3 mm mid-point displacement (Fig. 8). Since DSR cannot make adequate contribution to shear strength, similar brittle behavior of S800 is also observed on SX800 specimen (Fig. 9).

Thirdly, the load-displacement curves of S400, SX400 and R100 specimens are depicted in Fig. 10. Both in the specimens of S400 and SX400, the shear reinforcement ratio is increased very slightly with 400 mm stirrup spacing. However that ratio is also very insufficient according to the

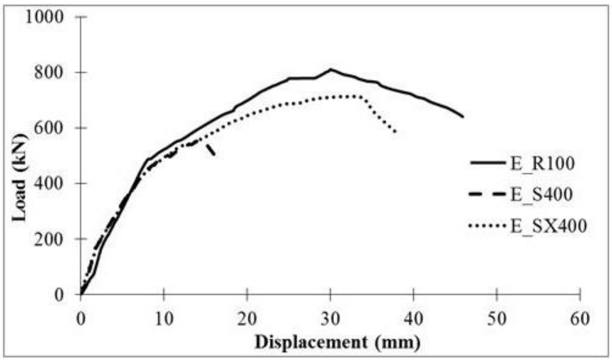

Fig. 10 Load-displacement curves of S400, SX400 and R100

seismic design code. Moreover, SX400 specimen includes additional DSR reinforcement diversely. In the test of S400 specimen, both flexural and shear cracks (at 142 kN) started to occur simultaneously. As the applied load was being increased, width of the shear cracks improved but propagation of the flexural cracks stopped. At the final stage, a sudden brittle shear failure was experienced at a load value of 557 kN with 14.4 mm mid-point displacement due to exceedance of shear capacity of the specimen (Figs. 10-11(a)). Additionally, in the test of DSR included specimen of SX400, firstly effect of DRS was observed on the initiation of crack pattern. Namely, flexural cracks (at 164 kN) occurred on the specimen first, hereafter shear cracks come into existence. Along with rise of the applied load, yield of tension reinforcement was observed. The maximum load level reached to a value of 712 kN with 33.1 mm mid-displacement (Fig. 10). Beyond that point due to the pin support condition, shear cracks widened and the specimen finally failed from exceedance of its shear capacity (Fig. 11(b)). The main contribution of DSR on behavior of the specimen is that an apparent significant increase in load and mid-displacement capacities of SX400 specimen is observed in a comparison with behavior of S400 specimen, as 27.8% and 129.8% respectively. It can be inferred from the propagation of flexural cracks that DSR increases shear capacity of the member and tension reinforcement work more efficiently. It supplies additional displacement capacity to the specimen as well. Moreover, it can be clearly seen from Fig. 10 that if both test results of S400 and SX400 specimens are compared with the results of reference R100, SX400 specimen including DSR represented rather similar behavior with R100 in terms of load-displacement behavior.

Finally, the load-displacement graphs of S200, SX200 and R100 specimens are shown in Fig. 12. Both in S200 and SX200 specimens, the shear reinforcement ratio is increased with 200 mm stirrup spacing. However that ratio is inadequate according to TSC-2007. SX200 specimen includes additional DSR reinforcement diversely. In the test of S200 specimen, both flexural and shear cracks (at 126 kN) started to be occurred concurrently similar to the behavior of S400 specimen. However, the number, width and length of flexural crack are increased crucially. As the applied load was being increased, width of shear cracks improved but propagation of the flexural cracks stopped. At

(a) S400

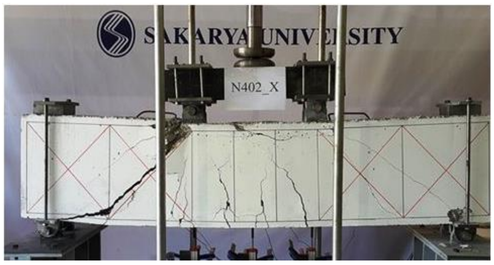

(b) SX400

Fig. 11 Test results of S400 and SX400

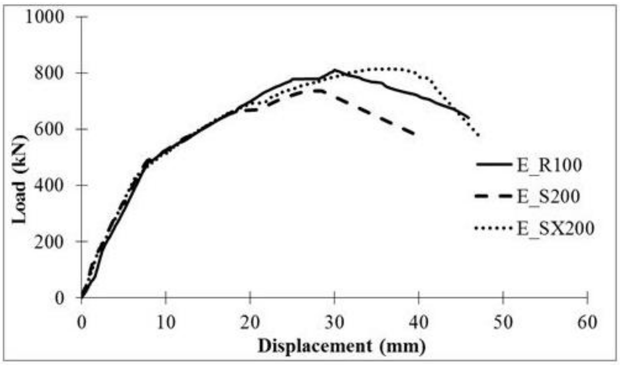

Fig. 12 Load-displacement curves of S200, SX200 and R100

the end, after exceedance of shear capacity of the specimen a shear failure was experienced at a load value of 737 kN with 28.2 mm mid-point displacement (Figs. 10-13a). Positive effect of stirrups on shear capacity of RC beams was experienced apparently in this specimen in a comparison with the previously tested S400 specimen. Additionally, in the test of SX200 specimen, a similar behavior of SX400 specimen was observed on the crack behavior. Namely flexural cracks (at 139 kN) occurred on the specimen first, hereafter shear cracks come into existence. Along with rise of the applied load, yield of the tension reinforcement was experienced. The maximum load level was achieved with a value of 814 kN with 36.9 mm mid-displacement (Fig. 12). Beyond that point due to pin support condition, shear cracks widened and specimen finally failed from exceedance of shear capacity (Fig. 13(b)). If the test results of S200 and SX200 are compared with R100 specimen, they represent very similar behavior in term of load-displacement. However, while the maximum load and displacement capacities of S200 are less than the reference R100 specimen, SX200 specimen catches successfully the behavior of the reference specimen in terms of load-displacement capacities and crack pattern. In spite

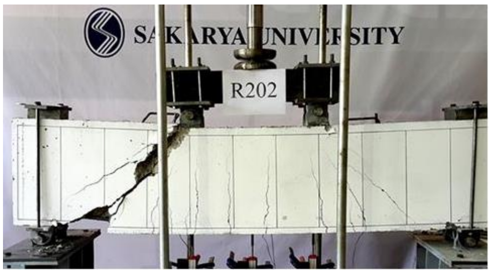

(a) S200

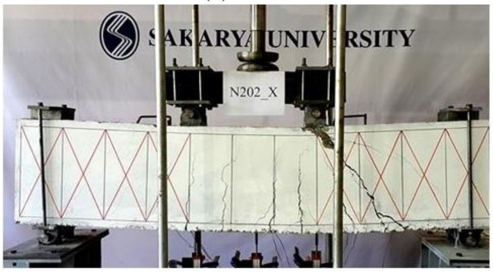

(b) SX200

Fig. 13 Test results of S200 and SX200

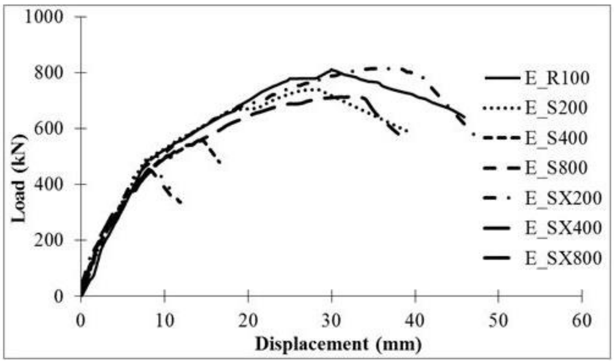

Fig. 14 Applied load - midpoint displacement curves of all experimental specimens

of the fact that SX200 specimen contains less stirrup then R100, the positive contribution of DSR on the shear capacity and ductility of RC short beams is also seen on the test results.

As a consequence of the experimental study, all of the test results are demonstrated in Fig. 14 and reported in Table 6. Since DSR is placed almost perpendicular to diagonal shear cracks, all specimens containing DSR prevent the widening of shear cracks. Therefore a significant improvement both in shear and displacement capacities of the members are experienced.

4.2 Numerical verification and parametric study results

In this part of the study, all tested specimens were simulated numerically according to the points described in the "Numerical Study" section above. In this process, specimens were verified sufficiently with the test results by using ABAQUS in terms of load-mid displacement behavior. Verification results of the numerical study and failure modes are tabulated in Table 7 and the load-mid displacement curves of all numerical models and test

Table 6 Experimental results

Specimen	Load (kN)				Displacement (mm)			Failure Mode
	Cracking	Yield	Peak	Ultimate	Yield δ_y	Peak	Ultimate δ_u	
E_S800	102	-	448	330	-	8,3	11,5	Shear
E_SX800	102	-	450	336	-	8,7	11,9	Shear
E_S400	142	452	557	480	8,4	14,5	16,6	Shear
E_SX400	164	457	712	580	8,5	32,7	37,0	Shear-Flexure
E_S200	126	485	737	586	7,7	27,8	39,3	Shear-Flexure
E_SX200	139	464	814	579	7,7	36,4	47,0	Shear-Flexure
E_R100	158	487	811	637	8,6	30,0	45,9	Shear-Flexure

Table 7 Numerical results

Specimen	Load (kN)			Displacement (mm)			Failure Mode
	Yield	Peak	Ultimate	Yield δ_y	Peak	Ultimate δ_u	
A_S800	-	482	416	-	9,0	13,5	Shear
A_SX800	-	519	460	-	9,0	14,5	Shear
A_S400	532	583	510	9,6	14	17	Shear
A_SX400	723	732	608	15	25	38	Shear-Flexure
A_S200	738	749	648	14	22	39,4	Shear-Flexure
A_SX200	787	872	636	16	20	48	Flexure
A_R100	793	808	631	17	24	45,7	Shear-Flexure

specimens are depicted in Fig. 15. In the table and figures, letters of A, R and S in entitles are abbreviations of ABAQUS, Reference and Specimen words respectively. Moreover, X demonstrates existence of DSR in the model, the integers of 100/200/400/800 represent the space of stirrups in millimeter.

When the table and graphs are evaluated, it is clear that both the load-displacement behavior of FE models and the tested specimens exhibit almost similar behavior. Therefore, it can be deduced that the numerical behavior of the tested specimens are successfully simulated with a sufficient accuracy. Nevertheless, the finite element models behave a little more rigid than the experimental results after yield of tension reinforcement. It may stem from the fact that the geometry, material, support conditions and load transfer mechanisms in finite element model are more perfect than the test specimens. Moreover, while test members have initial inner micro cracks, numerical models do not contain them (Mohamed *et al.* 2014). Hereafter, a parametric numerical study is conducted to investigate the efficiency of DSR. For this purpose, the numerical test results of SX200 and SX400 are taken into account as reference specimens, and the diameter and yield strength of DSR are selected as to be investigated parameters. Three different diameters and 2 different yield strengths of DSR are determined for the analysis as Ø8 mm, Ø10 mm and Ø12 mm, and 420 MPa and 500 MPa respectively. Results of the parametric numerical study are reported in Table 8 and demonstrated in Fig. 16.

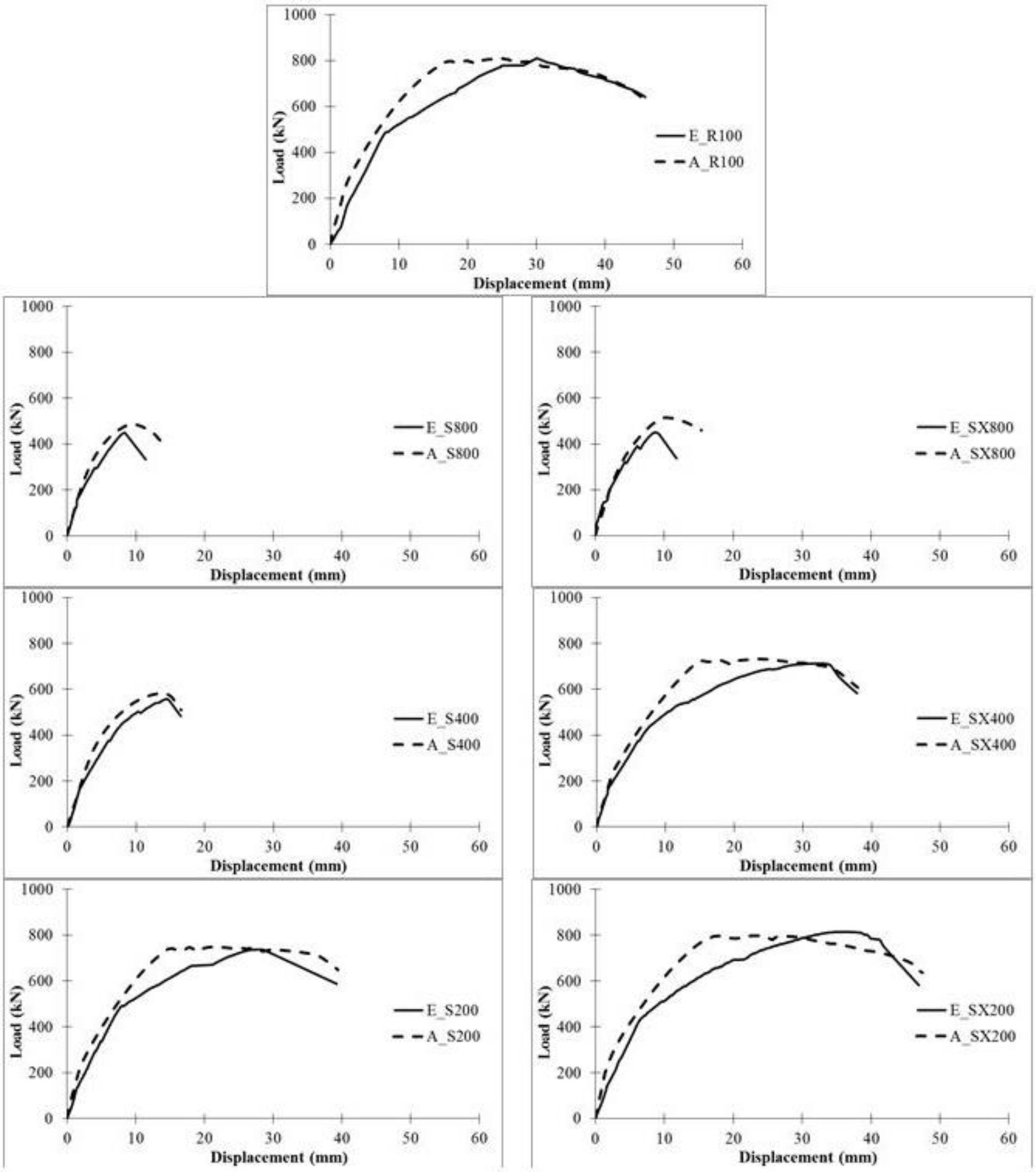

Fig. 15 Load-mid displacement curves of all numerical and test specimens

Table 8 Numerical parametric study results of DSR with different diameter and yield strength

Specimen	Yield Strength (MPa)	Ø8		Ø10		Ø12	
		V (kN)	Δ (mm)	V (kN)	Δ (mm)	V (kN)	Δ (mm)
A_SX200	420	797	47,5	843	93,8	880	100,6
A_SX400		733	38,0	780	78,2	808	86,5
A_SX200	500	833	93,6	879	100,0	906	122,3
A_SX400		758	42,1	797	97,1	835	113,4

If the results given in Table 8 and Fig. 16 are evaluated together, it can be concluded that increasing either the diameter or yield strength of DSR leads to a very significant increase in load-bearing and displacement capacities of RC short beams. Along with increase in both diameter and yield strength of DSR, flexure dominates the behavior of the members through initiation and propagation of flexural cracks. Especially, the specimens containing DSR with diameter of $\phi 12$ mm and 500 MPa yield strength represented very ductile behavior with 120 mm mid-displacement capacity. This behavior can be seen apparently from the numerical failure results of models in terms of equivalent plastic strain in uniaxial tension (PEEQT) that no shear cracks occurred on the specimens (Fig. 17).

If all numerical test results are being evaluated together to understand the main phenomena lying under the behavior of DSR since DSR is placed almost perpendicular to the diagonal shear cracks, it mainly prevents increase of crack opening widths. Moreover, it supplies very significant contribution to the shear capacity of the members. Therefore on the members sufficiently reinforced with DSR, the governing behavior shifts from shear to flexure resulting yielding of the bottom longitudinal bars. As a result, prevention of the propagation of shear cracks and yielding of longitudinal bars cause to achieve more ductile behavior on RC short beams.

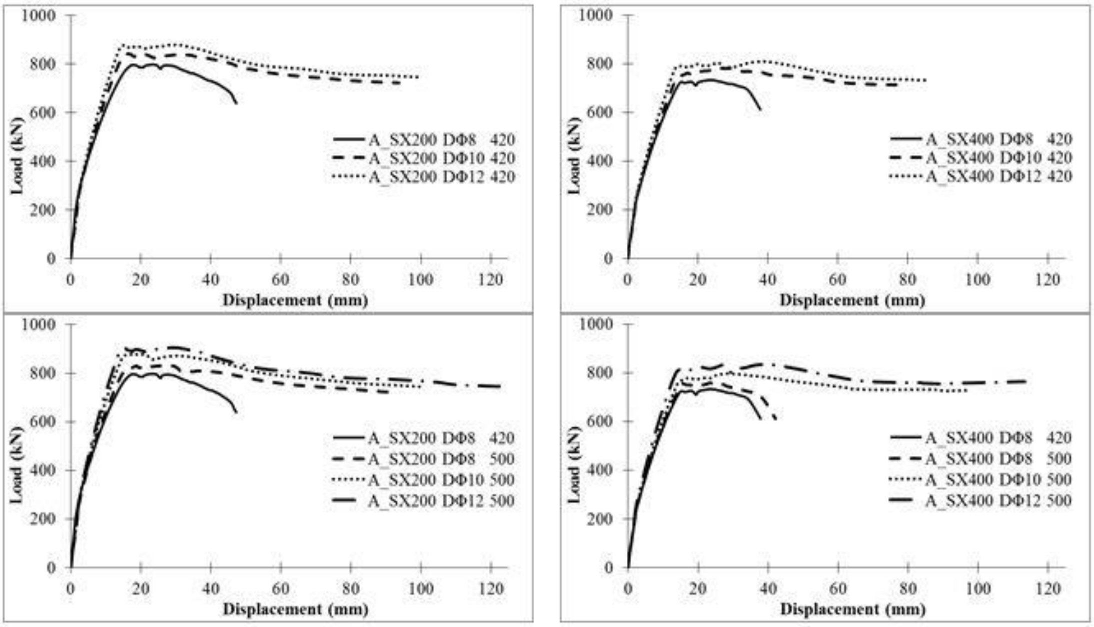

Fig. 16 Numerical load-displacement results of the parametric study

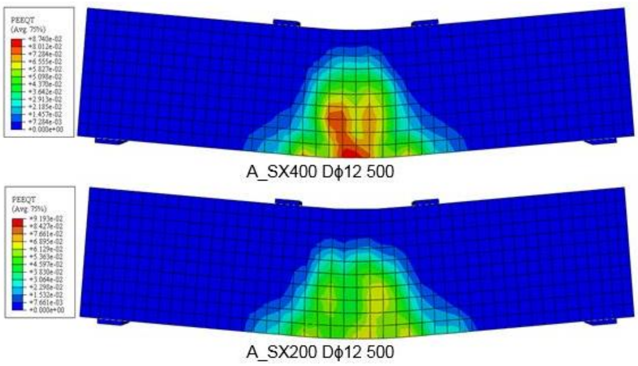

Fig. 17 Numerical failure results

5. Conclusions

The diagonal shear reinforcement (DSR) is numerically proposed as an easily applicable, economical and a new alternative shear reinforcement configuration in the literature to increase the shear capacity and ductility of RC normal beams, columns and beam-column joints. It is stated in those studies that not only DSR increases shear capacity and ductility of RC members significantly but also it works very effective under monotonic and cyclic loadings. Moreover, it makes a very significant contribution to the bond between concrete and steel reinforcement by reducing density of reinforcement. However, in an existing study, conducted on RC normal beams, the performance of DSR observed only numerically without an experimental study. Moreover, the scope of that study is only limited for RC normal beams. Because of that reasons in this study, an experimental and numerical study is performed to investigate the efficiency of DSR reinforcement on RC short beams which are shear critical RC members. For this purpose, 7 RC short beams were tested under a 4 point-loading test setup with a pinned support condition. Later a numerical FE study is conducted by using a FE-code ABAQUS. In the experimental study, together with increase of stirrup spacing, efficiency of existance of DSR on the specimens was observed. The effect of yield strength and diameter of DSR was investigated in the numerical parametric study. Analysis results were compared in terms of load-displacement behavior and failure modes.

According to the experimental and numerical parametric study results, DSR makes a very significant contribution to the shear capacity and ductility of shear critical RC short beams. Since DSR is placed almost perpendicular to the diagonal shear cracks, all specimens containing DSR prevent the widening of shear cracks. Therefore, a significant improvement both in shear and displacement capacities of the members are experienced. On the other hand, increasing either the diameter or yield strength of DSR leads to a very significant increase both in load-bearing and displacement capacities of RC short beams. Along with increase of both diameter and yield strength of DSR, the flexure dominates behavior of the members with initiation and propagation of flexural cracks. Especially the specimens containing DSR with diameter of ϕ12 mm and 500 MPa yield strength represent very ductile behavior with 120 mm mid displacement capacity.

The numerical simulations consisting of an accurate FE modeling technique and appropriate constitutive material models are quite reliable and robust tools to model the nonlinear behavior of RC members. Moreover, DSR would be an alternative strengthening technique for existing shear critical RC beams.

References

ABAQUS 2018 Research Edition. Abaqus Unified FEA. Dassault Systèmes SE: 10 rue Marcel Dassault CS 40501 78946 Vélizy-Villacoublay Cedex, France.

Al-Nasra, M. and Asha, N. (2013), “Shear reinforcements in the reinforced concrete beams", *AJER*, **10**, 191-199.

Chalioris, C., Favvata, M. and Karayannis, C. (2008), "Reinforced concrete beam-column joints with crossed inclined bars under cyclic deformations", *Earthq. Eng. Struct. Dyn.*, **37**, 881-897. https://doi.org/10.1002/eqe.793.

Chang, C., Kim, S.J., Park, D. and Choi, S. (2014), "Experimental investigation of reinforced concrete columns retrofitted with polyester sheet", *Earthq. Struct.*, **6**(3), 237-250. http://dx.doi.org/10.12989/eas.2014.6.3.237.

Corte, W. and Boel, V. (2013), "Effectiveness of spirally shaped stirrups in reinforced concrete beams", *Eng. Struct.*, **52**, 667-675. https://doi.org/10.1016/j.engstruct.2013.03.032.

Demir, A., Caglar, N., Ozturk, H. and Sumer, Y. (2016), "Nonlinear finite element study on the improvement of shear capacity in reinforced concrete T-Section beams by an alternative diagonal shear reinforcement", *Eng. Struct.*, **120**, 158-165. https://doi.org/10.1016/j.engstruct.2016.04.029.

Dirikgil, T. (2014), "Analytical and experimental investigation of new approaches to strengthening and designing of reinforced concrete columns", PhD Dissertation, Erciyes University Graduate School of Natural and Applied Science, Kayseri.

Dirikgil, T. and Altun, F. (2015), "Experimental study on effect of diagonal reinforcement details on hystretic behavior of RC short columns", *ICONSETE*, Vienna.

Ersoy, U. and Ozcebe, G. (2004), *Reinforced Concrete*, Evrim, Istanbul, Turkey.

Hibbitt, H., Karlsson, B. and Sorensen, E. (2011), ABAQUS User's Manual, Providence (RI), Dassault Systemes Simulia Corp.

Hu, Y., Jiang, L. and Zheng, H. (2017), "Cyclic tests and numerical study of composite steel plate deep beam", *Earthq. Struct.*, **12**(1), 23-34. https://doi.org/10.12989/eas.2017.12.1.023.

Karayannis, C. and Chalioris, C. (2013), "Shear tests of reinforced concrete beams with continuous rectengular spiral reinforcement", *Constr. Build. Mater.*, **46**, 86-97. https://doi.org/10.1016/j.conbuildmat.2013.04.023.

Lublinear, J., Oliver, L., Oller, S. and Onate, E. (1989), "A plastic-damage model for concrete", *Solid. Struct.*, **3**, 299-326. https://doi.org/10.1016/0020-7683(89)90050-4.

Luo, D., Ning, C. and Li, B. (2019), "Effective torsional stiffness of reinforced concrete structural walls", *Earthq. Struct.*, **16**(1), 119-127. https://doi.org/10.12989/eas.2019.16.1.119.

Mohamed, A., Shoukry, M. and Saeed, J. (2014), "Prediction of the behavior of RC deep beams with web openings using the finite element method", *Alex. Eng. J.*, **53**, 329-339. https://doi.org/10.1016/j.aej.2014.03.001.

Moretti, M.L. and Tassios, T.P. (2013), "Design in shear of reinforced concrete short columns", *Earthq. Struct.*, **4**(3), 265-283. https://doi.org/10.12989/eas.2013.4.3.265.

Nguyen, X.H. and Nguyen, H.C. (2016), "Seismic behavior of non-seismically designed reinforced concrete frame structure", *Earthq. Struct.*, **11**(2), 281-295. http://dx.doi.org/10.12989/eas.2016.11.2.281.

Panto, B., Giresini, L., Sassu, M. and Calio I. (2017), "Non-linear modeling of masonry churches through a discrete macro-element approach", *Earthq. Struct.*, **12**(2), 223-236. https://doi.org/10.12989/eas.2017.12.2.223.

TEC (2007), Turkish Earthquake Code, Ministry of Environment and Urbanisation, Ankara.

TS-500 (2000), Requirements for Design and Construction of Reinforced Concrete Structures, Turkish Standards Institute, Ankara.

Tubaldi, E., Barbato, M. and Dall'Asta, A. (2010), "Transverse seismic response of continuous steel concrete composite bridges exhibiting dual load path", *Earthq. Struct.*, **1**(1), 21-41. https://doi.org/10.12989/eas.2010.1.1.021.

Wang, P., Shi, Q.X., Wang, Q.W. and Tao, Y. (2015), "Experimental behavior and shear bearing capacity calculation of RC columns with a vertical splitting failure", *Earthq. Struct.*, **9**(6), 1233-1250. https://doi.org/10.12989/eas.2015.9.6.1233.

Wight, J.K. and MacGregor, J.K. (2012), *Reinforced Concrete Mechanics & Design*, Pearson Education Inc. New Jersey.

Yang, K., Kim, G. and Yang, H. (2011), "Shear behavior of continuous reinforced concrete T-beams using wire rope as internal shear reinforcement", *Constr. Build. Mater.*, **25**, 911-918. https://doi.org/10.1016/j.conbuildmat.2010.06.093.

KT